AOBA VELOX-IV: 2U CubeSat for the Technological Demonstration of Lunar Horizon Glow Mission

Sangkyun Kim[a,*], Necmi Cihan Orger[a], Jose Rodrigo Cordova-Alarcon[a], Marcos Hernadez-Herrera[a], Hirokazu Masui[a], Takashi Yamauchi[a], Kazuhiro Toyoda[a], Mengu Cho[a,b]
Bui Tran Duy Vu[b], Tran Quang Vinh[b], Lim Wee Seng[b], Cheng Tee Hiang[b]

[a] *Kyushu Institute of Technology, Japan*
[b] *Nanyang Technological University, Singapore*

[*] Corresponding author
Email address: kim.sangkyun571@mail.kyutech.jp (Sangkyun Kim)
URL: https://kyutech-laseine.net/english/ (Sangkyun Kim)

Abstract

AOBA VELOX-IV is a 2U-sized CubeSat that has been developed by the Kyushu Institute of Technology and Nanyang Technological University for the technological demonstration of a future lunar mission. Decades ago, Surveyor and Apollo programs reported light scattering observations on the horizon of the Moon; however, only a limited number of investigations were performed after the Apollo program to observe the lunar horizon glow (LHG). It is still unknown what conditions produce the light glow on the horizon of the Moon. The lunar mission of the AOBA VELOX project is planning to send CubeSats to the Moon and to capture images of the LHG on the lunar orbit while determining the conditions that can support light scattering above the lunar horizon. Before the satellites go into the lunar orbit, the necessary technologies must first be confirmed in Earth orbit. AOBA VELOX-IV was launched to low earth orbit via a JAXA Epsilon rocket in 18th January 2019. This paper explains the LHG mission first, and presents an overview of AOBA VELOX-IV, its payloads, technical issues, and the flight model.

Key words: Lunar horizon glow, Small satellite, CubeSat, Pulse plasma thruster, AOCS, Technological demonstration

---

1. Introduction

The lunar surface is covered with a soil-like layer that is composed of large rocks, boulders and particles with sizes from several centimeters to sub-micrometer [1,2], and the lunar regolith material is produced due to micrometeorite impacts and space weathering processes with a wide range of

particle sizes and properties. Even though the size range of the lunar dust is not clearly defined, it is generally considered to comprise particles smaller than 20 μm in diameter, and there are four noteworthy shapes of lunar dust grains, i.e., spherical, angular blocks, glass fragments, and irregular, according to electron microscopy scanning images [3]. In addition, the lunar dust was anticipated before the Apollo missions [4], and the particles could be transported above the lunar surface through several physical mechanisms, such as micrometeorite impacts, electrostatic repulsion, potential moonquakes, and surface activities during robotic and human missions.

Lunar Horizon Glow (LHG) is the forward-scattering of the sunlight above the lunar terminator, the border line between day and night, and it was first reported by the Surveyor program of 1966 [5]. In addition, Apollo astronauts reported that they had witnessed the horizon glow as well [6], and it has been suspected that electrostatically lofted lunar dust grains scattered the sunlight above the surface near the terminator region. The lofted dust has been explained by the surface charging of the Moon under the solar wind, seen in Fig. 1. As the Moon has no atmosphere, the lunar surface is directly exposed to plasma, and the lunar surface is electrically charged as a result of photoelectron emission due to the solar UV and X-ray emissions, and the interaction with solar wind and/or Earth magnetosphere plasma. The surface charging is not uniform, especially near the terminator of the border between day and night, where a relatively strong electric field could transport the lofted dust particles to higher altitudes. Furthermore, the laboratory experiments have demonstrated that dust grains can be lofted from a dusty surface due to charging within microcavities by the emission and re-absorption of electrons on the patch surfaces facing the small-scale gaps between the dust grains [7–9]. Simulations predicted the heights of 0.1-μm radius dust grains are approximately 200 m under a regular solar wind, and these heights increase up to approximately 540 m under solar wind-like plasma density and enhanced electron temperature for less than an hour during a post-shock plasma passage during a coronal mass ejection event [10].

Since the Apollo era, several attempts have been made to observe LHG. Forward-scattering of sunlight was searched for by the Clementine star tracker navigation cameras in order to observe high-altitude LHG like that observed by Apollo 15. However, LHG was not detected during these measurements [11]. In addition, a Lunar Reconnaissance Orbiter (LRO) LAMP UV spectrograph also could not measure the dust densities that could explain an excessive brightness above the lunar terminator region. The Lunar Atmosphere and Dust Environment Explorer (LADEE) mission measured dust particles between 3 and 250 km altitudes, and the results showed that the dust densities of 0.1-micron–sized grains similar to those in LHG observations were not present above the lunar horizon [12,13]. Currently, the exact conditions near the lunar surface, as well as the upstream plasma that can produce LHG, are unknown.

To reveal the mystery of LHG, the main problem is that the number of observation attempts has been considerably limited. One idea to increase the number of observations is to put multiple satellites around the lunar orbit and capture as many terminator images as possible. And, small satellites such as CubeSats can be a good solution. In recent years, several lunar missions have been proposed, followed by the augmented interest in the investigation of the lunar environment and surface composition. CubeSat missions, such as Lunar Flashlight, Lunar IceCube, LunaH-Map, SkyFire and OMOTENASHI, are being developed to conduct exploration missions by analyzing the lunar surface and radiation environment [14].

Before jumping to the lunar mission, however, the necessary technologies for LHG observation mission should first be demonstrated in Earth orbit. The Moon's orbit has very different characteristics from Earth orbit, with an extremely low magnetic field and a highly irregular gravity field. Because of the extremely low magnetic field, a magnetic torquer cannot be used as is done with satellites in Earth orbit. Usually, momentum dumping of reaction wheels is necessary. A satellite propulsion system is also required to maintain the satellite altitude against the irregular gravity field for as long a mission lifetime as possible. For the future design of an imaging mission system, images of the horizon are to be checked under low light conditions [15].

Because of these requirements, the Kyushu Institute of Technology (Kyutech) and Nanyang Technological University (NTU) jointly developed a 2U CubeSat named AOBA VELOX-IV (AV4) to verify, in Earth orbit, the necessary technologies for a lunar mission. Its primary payload is the Pulse Plasma Thruster (PPT) of an electrical propulsion system. In our current design, the PPT is the only actuator for momentum dumping of reaction wheels and orbit maintenance in the lunar orbit. Also, a small commercial camera is installed as a payload to check the imaging function of the horizon. Besides these payloads, the required attitude control and orbit maintenance functions will be checked in Earth orbit. AV4 was selected as one of the piggy-back satellites to be launched by an Epsilon rocket under the framework of the Innovative Satellite Technology Demonstration Program of JAXA. The satellite flight model was delivered to JAXA in September 2018. The satellite was launched to the 500-km Sun-synchronous orbit in 18th January 2019, and is still under initial operation to check basic functions.

The purpose of this paper is to present an overview of the AV4 project, from mission requirements to the flight model. Small satellites are already playing an important role in space engineering applications, even though they have very limited resources. And their application is now being extended to deep space exploration. This overview aims to explain and share information regarding how we developed a 2U CubeSat for the technological demonstration of a lunar mission with its limited resources. This paper consists of seven parts. Section 2 explains the mission requirements of LHG observation, and the mission success criteria for the AV4 satellite project target. Section 3 presents an overview of the AV4 CubeSat,

and section 4 presents the payload of the mission system. Section 5 briefly explains the function of an Attitude and Orbit Control System (AOCS). Section 6 presents the AV4 flight model, and section 7 offers the conclusions of this work.

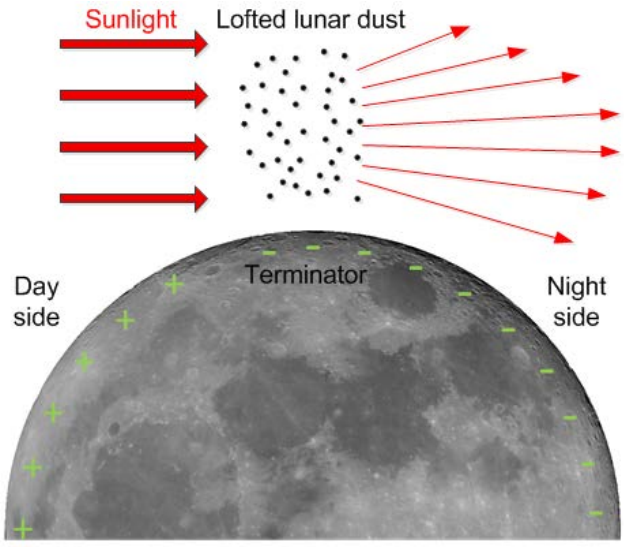

Fig. 1 Schematic of Lunar Horizon Glow, LHG

2. Mission requirements

2.1 Glow observation

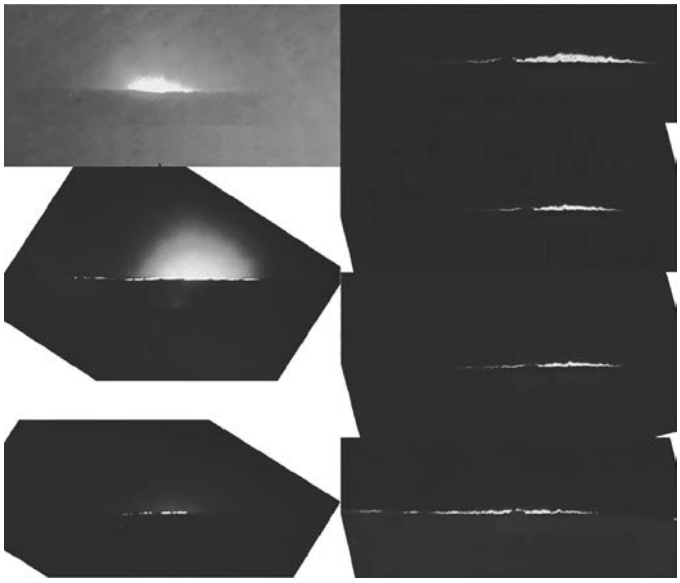

Fig. 2 LHG detected by TV cameras of the Surveyor 5, 6, and 7 landers [5]

Surveyor onboard TV cameras monitored the western horizon above the lunar terminator, and they achieved the first observations of LHG in 1966 and 1968, shown in Fig. 2, prior to the Apollo missions. Furthermore, image analysis indicated that LHG was produced due to the forward-scattering of the sunlight by

dust grains with a radius of 5–6 μm reaching up to an approximately 30-cm height while following the passage of the lunar terminator [5,16]. Since the abundance of dust particles was particularly higher than the ejecta produced by micrometeorite impacts, electrostatic dust transportation was suggested as the responsible physical mechanism. Surveyor 7 started to monitor LHG earlier than the other missions, and it detected the highest brightness level, since the lunar terminator was in close proximity to the spacecraft. The brightness gradually decreased, since the lunar terminator was continuously moving away.

Following the Surveyor missions, Apollo 15 orbital image sequences detected an excessive brightness over the lunar horizon while orbiting at around a 100-km altitude [6,17,18]. In addition, Apollo 17 astronauts sketched some of the observations that indicated the presence of a very fine component of lunar dust up to approximately a 10-km altitude, as shown in Fig. 3. These observations can be called "high-altitude LHG." It is a highly variable phenomenon, since there was no trace of excessive brightness to the Coronal Zodiacal Light (CZL) by the interplanetary dust particles during Apollo 16 attempts to observe light scattering. In addition, the responsible dust particle sizes during the Apollo missions are estimated to be submicron, of 0.1–1 μm in radius. The blue line in Fig. 3 shows the boundary of LHG, whereas the red line shows the boundary of light scattering by the interplanetary dust particles of CZL.

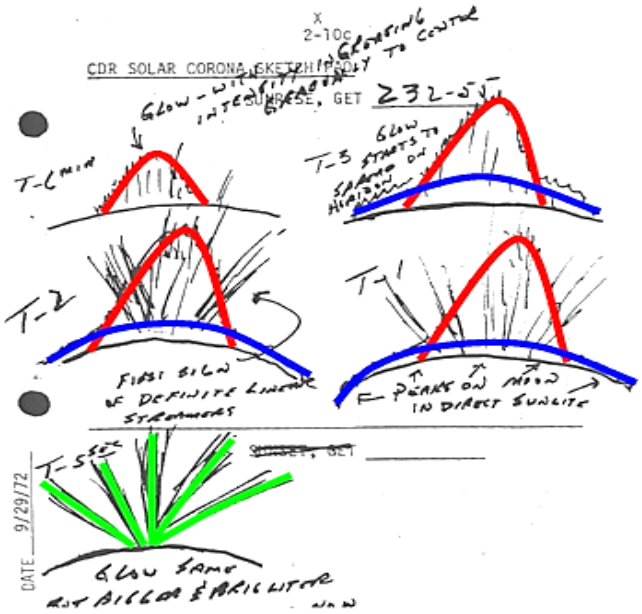

Fig. 3 A sketch by Apollo 17 astronaut Eugene Cernan [18]

The differences between the Surveyor and Apollo LHG observations are the results from a dust population that varies in particle size and density at different heights, as shown in Table 1. First, the brightness levels are higher in the Surveyor observations since the responsible dust grain sizes are ~5–60 times larger near

the surface than those for the high-altitude LHG estimations. Therefore, they can more strongly scatter sunlight with sufficient dust density. In addition, Surveyor missions were able to observe LHG for longer periods of time, since they monitored the terminator region that accommodated electrostatically transported dust particles while shifting westward at approximately 15 km/h during a sunset along the equator [19,20]. On the other hand, high-altitude LHG was observed for a short period of time from the orbit with lower brightness levels, due to particle sizes as small as ~0.1–1 μm [21]. Since the presence of CZL would potentially overlap with this brightness, it represents a challenge to distinguishing the source of the high-altitude LHG. As a result, a luminous event less than 20 lux needs to be captured by a sensor with high sensitivity, and the image spatial resolution needs to be much less than 1 km in order to detect the gradually decreasing brightness levels above the lunar terminator.

Table 1. Comparison of LHG Observations in General Terms

Mission	Position	Evidence	Time Period	Responsible Dust Grain Size	Height of Dust Cloud	Observed Luminosity Levels
Surveyor	Lunar Surface	Onboard TV camera images	0.5 to 2.5 hours	5 to 6 μm	10 to 30 cm	60 to 2600 lux
Apollo	Lunar Orbit	Drawings and Images	Several minutes	0.1 to 1 μm	1 to 10 km	0.2 to 20 lux

In the lunar mission, the imaging payload shall be a monochrome low-light Commercial Off-The-Shelf (COTS) camera with a proper interface. The technology demonstration of the payload will be performed in LEO orbit. During the Earth mission, the camera will be used for Earth-rim imaging as well as observations of night view. For the night view imaging operation, the brightness requirements are selected by investigating various areas, because the light densities of different cities are related to the urbanization and their landscape. Recently, an aerial night photography operation was performed to investigate the brightness levels for different landscapes [22], and these values showed that low-light imaging performance of the camera module in space can be tested by night view imaging before the lunar mission. The camera payload requirements are listed in Table 2.

Table 2. Camera Payload requirements

Specification	Requirement
Mass	< 0.2 kg

Volume	< 0.07U, U = 10 cm x 10 cm x 10 cm
Maximum Resolution	VGA
Sensor Type	CMOS (with low noise) or CCD (with low power consumption)
Field of View	>40^{o}
Minimum Luminosity	0. 015 Lux
Sensitivity	3.0 V/Lux-sec and higher
Exposure Time	0.033 s
Operation Temperature Range	-10 to 50^{o}C
Interfaces	UART, SPI, I2C

2.2 Attitude and Orbit Control

There are several ways to put a spacecraft on the lunar orbit. One way is to use strong propulsion system of its own, and do the orbit maneuver from earth orbit to lunar orbit as like Beresheet of SpaceIL. However, this is extremely hard way for CubeSat program, actually the lander of Beresheet had 585[kg] of mass, but 435[kg] of the mass was for fuel. Another way is to use piggyback launch service of deep space exploration program. At that case, CubeSat needs to have propulsion system for the trajectory correction to the moon after deployment from rocket, and for the deaccelerations of its speed near the moon for the lunar capture maneuver. 6U CubeSat of JAXA's OMOTENASHI program chose this way using the secondary payload service of SLS(Space Launch System), NASA. If AOBA VELOX satellite can use any deployment service from lunar orbiter, it is the best way to save the fuel of propulsion system for the longer mission lifetime, even it is very rare chance in near future. At this study, the propulsion system of AOBA VELOX-IV is analyzed for the orbit maintenance work only assuming it takes enough low altitude orbit already by the maneuver.

In future lunar missions, the AOCS will perform the task of pointing towards the moon horizon to capture images of LHG. When the satellite is not in mission mode, the AOCS keeps the attitude pointed towards the sun for maximum power generation, and periodically performs orbit maintenance to increase the mission lifetime. The AOCS aligns the thrust vector to the direction of satellite movement for the orbit maintenance work. Reaction wheels are the usual actuators for attitude control, but a reaction wheel needs another actuator to dump momentum when the wheel has reached the saturation point of its momentum. As the moon has a very low magnetic field, a magnetic torquer, a favorite choice for CubeSats, cannot be used. Therefore, the thruster is used not only for orbit maintenance but also for the attitude control actuator.

The Moon possesses a very irregular gravity field that can shorten the mission lifetime of any satellite orbiting it, particularly at low altitudes. The reason is that

the Moon has several strong gravity points near the equator. When the satellite has some specific small inclination angle, it has many chances to pass through the strong gravity area, and loose its altitude rapidly. Thus, orbital analysis should be performed utilizing an accurate lunar gravity potential model. Nowadays, better spherical harmonic resolutions of the lunar gravity potential model are available after the measurements obtained by the Clementine, Lunar Prospector Discovery, SELENE and GRAIL missions [23]. Frozen orbits which feature a quasi-periodic behavior in three-dimensional space [24], and where one or more orbital parameters are held constant, are the best option for long-term missions [25]. However, a lunar mission for LHG requires a low altitude of ~100 km. Also, as small satellites are usually deployed as piggybacks on larger missions, their deployment into a frozen orbit is not guaranteed. Thus, the utilization of propulsion systems becomes very important for the extension of mission lifetime in a low lunar orbit.

In Fig. 4, the mission lifetime of a satellite orbiting the Moon at an initial 100-km-altitude circular orbit is shown, which was obtained by solving the restricted three-body problem [26] in a MATLAB-Simulink simulator. The simulation used a zero-degree condition for the right ascension of the ascending node, and the value of the argument of perigee is also set to zero degrees. The simulation used the optimal in-plane orbit maneuvers strategy [27,28] to mitigate the variation of the eccentricity and periapsis, due mainly to the irregularity of the Moon's gravity field, and to keep the altitude of the spacecraft within 100 km. Regarding the spacecraft parameters, we have considered a spacecraft with a mass of 2.8 kg, 4.57 x 10-6 N/m^2 solar radiation pressure, c_r=1 reflectivity from a black body, and 0.02 m^2 area exposed to the Sun. Very interestingly, mission lifetimes are dramatically different depending on the inclination angle of the orbit condition. Some inclination angles satisfy a mission lifetime of more than one year without any orbit maintenance, while some angles show an extremely short lifetime, sometimes less than 15 days. The best way is to avoid the inclination angles known to lead to a short lifetime and choose one associated with a long mission lifetime. However, when the inclination angle cannot be fit to the angle of the best condition, even a small amount of PPT propulsion power can extend the mission lifetime. Figure 4 shows the changes in mission lifetime when the satellite is under various ΔV conditions from 0 m/sec to 120 m/sec.

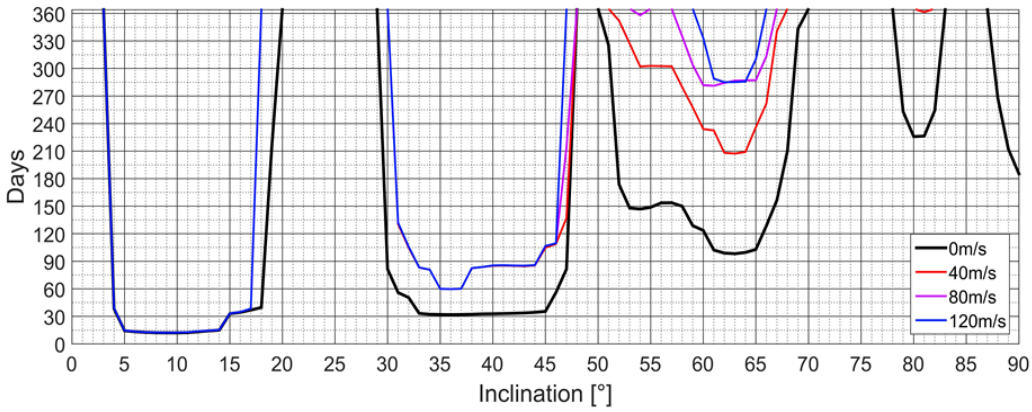

Fig. 4 Mission lifetime with inclination angle and orbit maintenance

The expected lifetime mainly depends on the inclination angle condition. However, if the inclination angle is large enough, the PPT orbit maintenance maneuvers successfully increase the mission lifetime from several days to more than a year, despite orbital disturbances due to the irregular gravity field of the Moon. These results show that a small satellite deployed into the unstable regions of an inclination angle can overcome the unstable orbit condition by performing orbit maintenance maneuvers using PPT. And this can allow for a longer lunar mission lifetime, increasing the possibilities of a successful LHG mission.

For the AV4 mission, this orbit maintenance function will be demonstrated for the verification of the AOCS. Current plan is to generate ΔV after the PPT performance is confirmed by the momentum dumping of the reaction wheel. During the operations of the orbit maintenance demonstration, the satellite signal will simultaneously be checked by multiple ground stations to find the accurate position. Natural decay of a satellite depends on the perturbation of the orbit condition at that time, and the satellite position will be checked against the natural decay position.

2.3 Mission success criteria

To demonstrate the feasibility of using a CubeSat platform in a future lunar mission, the following AV4 mission success criteria should be accomplished in Earth orbit:

- Momentum dumping of 0.0001-Nms angular momentum via PPT within 1 h
- Orbit maneuvering via PPT with ΔV=60 m/s within 1 year
- Capturing several images of the horizon in sequence while passing from the day side to the night side
- Capturing Earth night view images via the mission camera

3. Satellite Overview

Table 3 lists the specifications of AV4, a standard 2U CubeSat. The satellite bus was developed by NTU to meet JAXA mission requirements and safety regulations.

Table 3. Satellite specifications

Dimensions (Stowed)	113 mm x 113 mm x 227 mm
Dimensions (Deployed)	474 mm x 113 mm x 227 mm
Mass	2,520 g
Orbit	Sun-synchronous 500-km orbit
Design lifetime	24 months in LEO
Attitude and orbital control	3-axis gyroscope, 2 fine sun sensors with 120° FOV, 6 coarse sun sensors, 3 reaction wheels, and 1 pulsed plasma thruster for 2-axis angular movements
On-board data handling	On-board computer with 2-Gb storage, UART and I2C data interfaces
Communication	UHF half duplex 4800-bps GMSK downlink/uplink, dipole antenna
Power	4 deployable and 2 body-mounted solar panels for 18-W peak BOL 5.8 Ah Li-Ion battery at 7.2 V nominal
Structure	Al. 7075-T7351 chassis with stainless steel load-bearing parts
Thermal control	Battery heaters
Payload	PPT, Camera

Figure 5 shows the satellite external overview when it deploys the two deployable solar panels. The satellite maintains the sun pointing control to point the –X surface of major solar cells toward the Sun during the sunlit time after the panels are deployed. Each surface has a coarse sun sensor to detect the direction of the Sun. Especially, the -X surface of major power generation and the –Z surface of the mission camera have fine sun sensors for accurate Sun vector information. The gyroscope is installed to measure the angular velocity of the satellite. For the primary actuator, three reaction wheels developed by NTU were installed. PPT will be used for the momentum dumping of the reaction wheels and orbit maintenance demonstration, and it is installed on the +Z surface with four heads. The power system and communication system are the core parts of the satellite and need to be designed with high reliability. The communication system and solar cell panels are selected with heritage on the small satellite market, and the battery is screened and assembled at Kyutech with caution.

It was challenging to design AV4 for all the requirements, given the very limited resource of a 2U CubeSat. And the design must also satisfy all of the safety issues. The designing of the deployable components, the UHF antenna and the solar panel, especially, had many problems to be solved. The most difficult problem was complying with JAXA's safety requirements. Modifying the UHF antenna deployment was particularly difficult as it was a catalog product from a market vendor. The company was not willing to modify the design according to JAXA's recommendations. The antenna deployment must have multiple inhibits to prevent accidental deployment during launch. To meet that requirement, it was decided to hold the two antennas by the solar panels. As the solar panel was designed in-house, it was possible to implement the design change to have multiple safety inhibits. The deployment system uses a heat knife and polyethylene string, and its polyethylene string passed several of JAXA's regulation tests to avoid the risk of a hazard. Another safety concern was high-voltage shock due to the PPT. Therefore, the injection port size of the PPT head was designed so that nobody could accidentally touch the high-voltage part of the PPT. Figure 9 is an external view of the actual flight model when it was undergoing an environmental test in June of 2018.

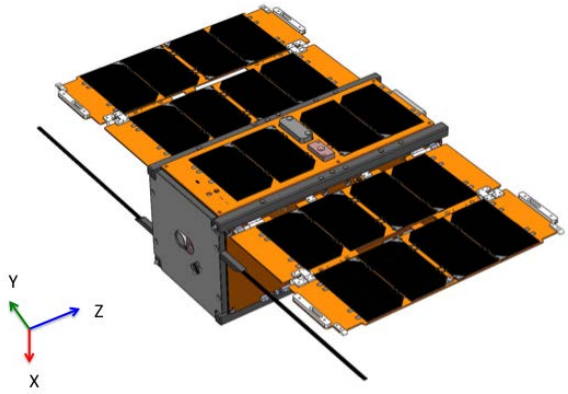

Fig. 5 Satellite external overview after panel deployment in orbit

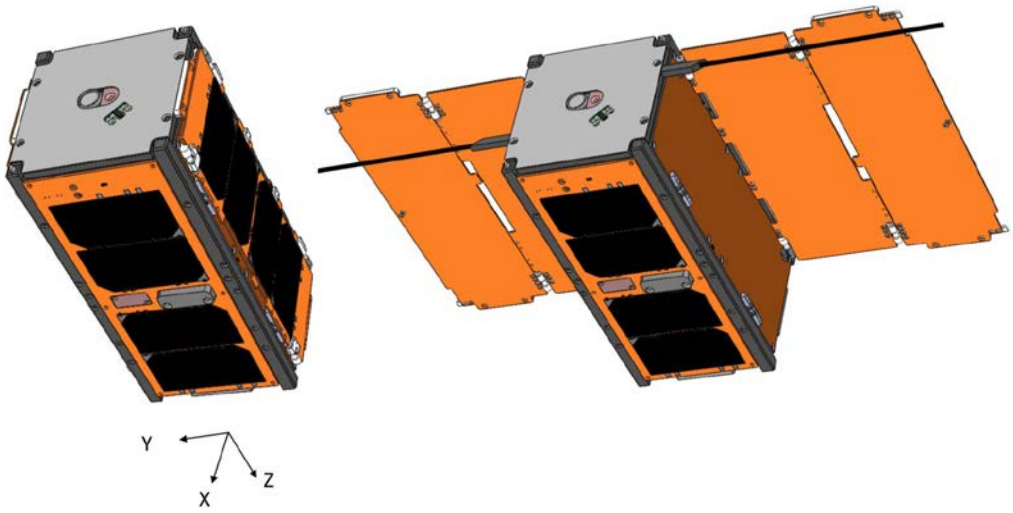

Fig. 6 Satellite external overview in the stowed and the deployed conditions

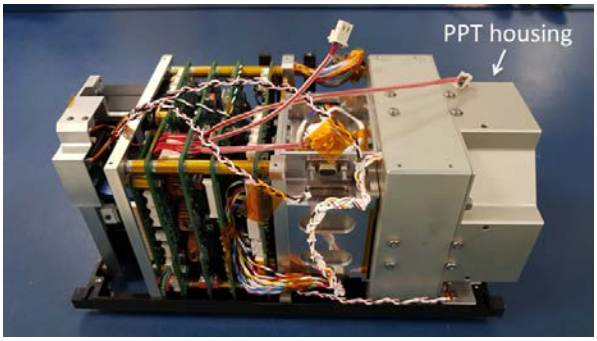

Fig. 7 Internal view of AOBA VELOX-IV

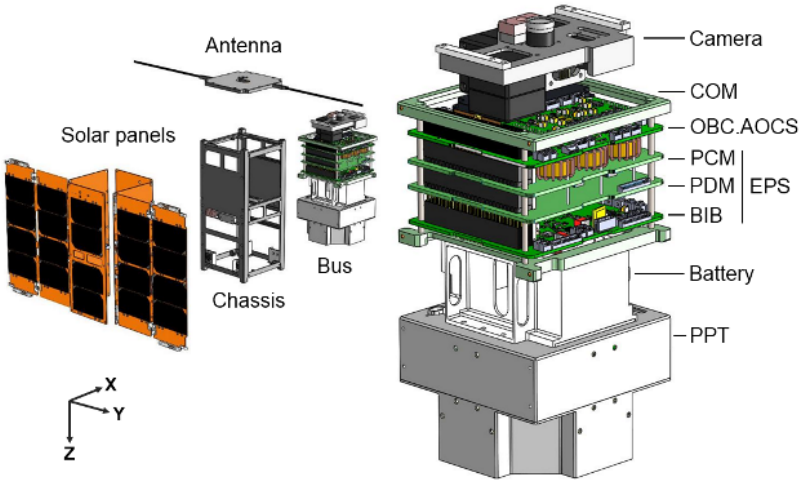

Fig. 8 Internal structure of AOBA VELOX-IV

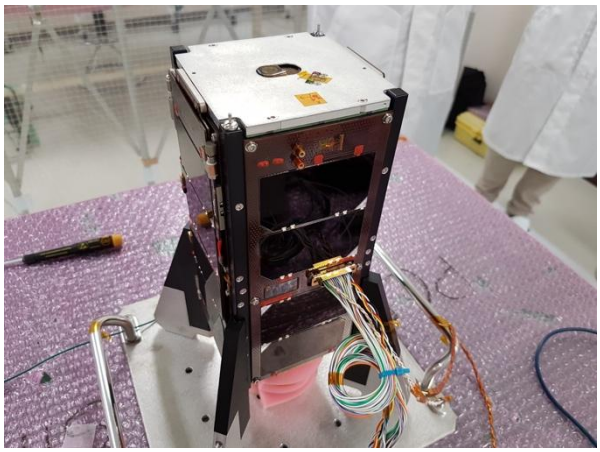

Fig. 9 External view of flight model

4. Payloads

4.1 Pulse plasma thruster

The most important mission of AV4 is to verify a 4-head PPT in Earth orbit. It is designed not only for the momentum dumping of reaction wheels during attitude control task, but also for satellite orbit maintenance demonstration. Table 5 lists the specifications of the PPT. In Fig. 10, we can see the PPT module and Fig. 11 shows the engineering model PPT fired in a vacuum chamber. The test fired the PPT for 2 hours in the chamber accumulating 7200 shots of operation for each thruster head.

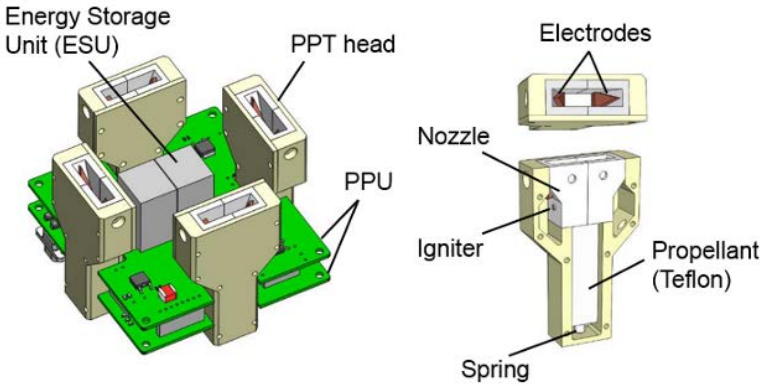

Fig. 10 PPT module and its head

The impulse bit I_{bit}, specific impulse I_{sp} and mass bit m_{bit} have been measured to assess the PPT design and must meet the mission requirements. An in-house-developed micro-Newton thrust stand, shown in Fig. 11, was used to measure the impulse bit of the PPT. The torsional arm length is pre-defined as 0.5 m. The pivot is a Riverhawk 6012-400 flexural pivot. This stainless-steel frictionless pivot had a torsional spring rate of 0.0434 Nm/^{0} and displayed significant advantages over conventional bearings—lubricant free, vacuum compatible and resistant to thermal stress. A linear displacement sensor is installed using an ILD 2300-2 Micro Epsilon optical sensor. This sensor operates based on the principal of triangulation, non-contact and non-intrusive nature and has a measuring range of 2 mm with 30-nm resolution. Moreover, a passive magnetic damper is used to dissipate the kinetic energy of the stand after perturbation in order to bring the stand to rest and prepare it for the next measurement. The characteristics of the thrust stand are summarized in Table 4.

Table 4. Thrust stand specifications

Parameters	Specification
Natural Frequency	0.819 Hz
Sensitivity	4.56 μN/μm
Noise	0.12 μm
Zero drift	0.15 nN/s
Resolution	0.55 μN

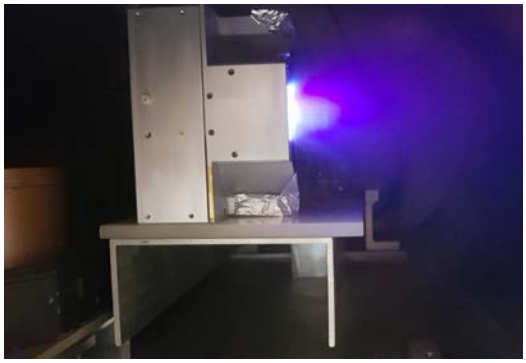

Fig. 11 Photograph of PPT firing in a vacuum chamber

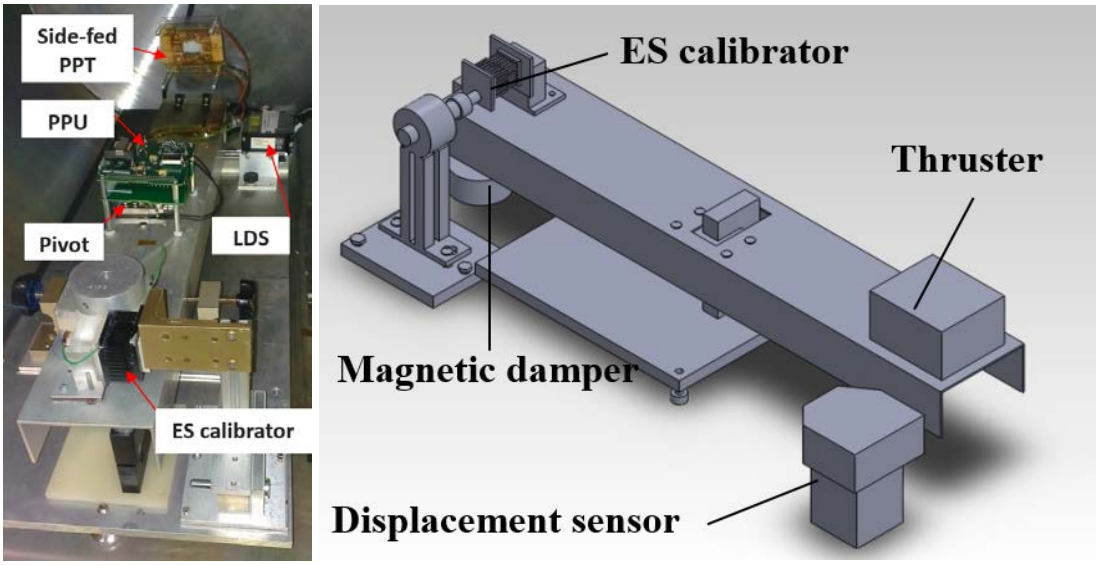

Fig. 12 Thrust stand setup

Figure 13 shows the four PPT heads in the actual flight model. PPT generates an arc between anode and cathode, and accelerates a small amount of fluorocarbon-based propellant. This plume can make trouble of contamination to the sensitive devices, and several researches surveyed its risk of contamination [31]. In the design of AV4, PPT is installed on the surface of +Z, and the mission camera of optical payload is installed on the opposite surface of -Z to minimize the risk of contamination.

PPT has to provide with the function of momentum dumping for all reaction wheels of three axes when the spacecraft goes to the lunar mission actually. However, the PPT of AV4 provides torque for the momentum dumping of reaction wheels of the X and Y axes only, and additional actuator is also not installed because of the critical space limitation. The Z axis has no torque from PPT, and momentum dumping of the reaction wheel is not possible. Because of that, the attitude control system was designed not to reach saturation of the reaction wheel for at least the first month. The basic mission plan is to test all AV4 functions before the Z axis reaction wheel momentum becomes saturated. However, even if the reaction wheel of the Z axis becomes saturated, all missions can be tested with

reduced efficiency. The PPT will also be examined for the feasibility of the orbit maintenance function.

Table 5. PPT Specifications

Parameter	Specification
Capacitor bank, C_b	3 μF/2000 V
ESU voltage, V_c	1200 V
Firing frequency, f_r	1 Hz
Electrical power, P_{in}	2.25 W
Mechanism	Breech-fed
Size	97.5 x 97.5 x 70.0 mm
Impulse bit, I_{bit}	25.203 μNs
Mass bit, m_{bit}	3.8 μg
Total mass of Teflon fuel block, m	22.88 g
Specific impulse, I_{sp}	676 s
Exhaust velocity, v_e	6.632 km/s

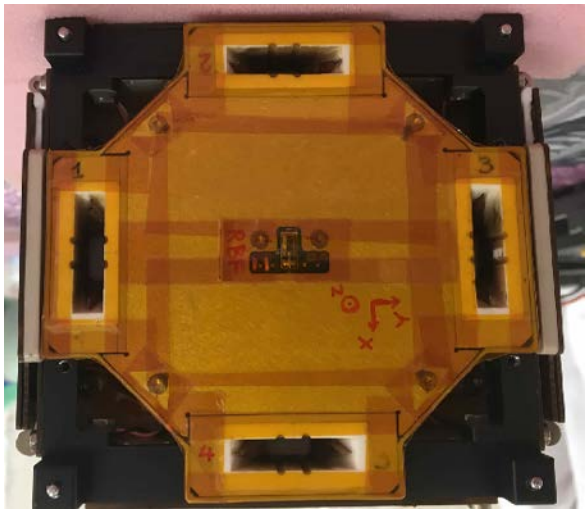

Fig. 13 PPT heads on the flight model

4.2 Camera

Many COTS cameras have been considered as candidates; however, the interface and light sensitivity requirements eliminated most of the candidates at the beginning. The power consumption and size requirements were effective for selection as well. There are also several options for the lens, and they are compared according to their F-numbers, field of view (FOV) and IR cut filters. For the mission, a lower F-number, wide FOV and IR cut filter are preferable choices. In addition, the height of the lenses must be considered because of the size

limitations, and too wide FOV angles will cause distortions in the image plane, which can affect the horizon detection performance. According to the selection process, the payload has been determined to be a C329BW camera module for this mission, and the selected lens is a BB270 model. The specifications can be given in Table 6, and Fig. 15 shows the development board of the mission camera.

Table 6. Camera Specifications

Camera	C329BW
Resolution	640 x 480
Sensor Type	1/4" OmniVision VGA sensor
Sensitivity	3.8 V/lux-sec
Power Consumption	264 mW
Mass	6 g
Size	20 x 28 x 25 mm
Interface	UART
Sensor S/N Ratio	50 dB
Dynamic Range	60 dB
F-number of lens	1.6
Field of view	43 degree
Filter of lens	IR cut
Height of lens	20 mm
Cap diameter of lens	14 mm

The camera module performs compression of raw images for efficiency of operation, and the image size is approximately reduced from 307 KB to 30 KB, a roughly 90% reduction of image size. And it can be interfaced with an OBC by UART. It has a power supply pin, data transfer and receive pins, and a ground pin, as shown in Fig. 14. In addition, the OV529 Serial Bridge has a Jpeg converter and controller chip that receives raw images from the camera sensor and compresses them before sending them to the OBC. It also has a very low power consumption of 80 mA in active status.

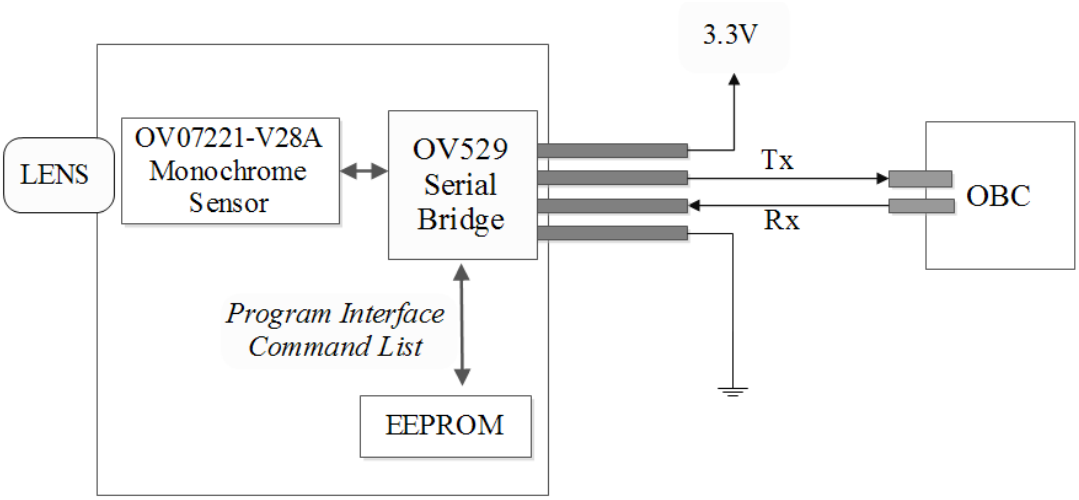

Fig. 14 Basic Schematics of the Camera Interface

The camera payload integrated into the flight model, shown in Fig. 17, passed the environmental test. Sufficient robustness to withstand vibration and shock environments of launch service was confirmed. Figure 16 shows a sample picture taken by the integrated camera payload.

Figure 15 Camera selected for the AV4 mission and development board

Fig. 16 Sample photograph taken by the camera payload

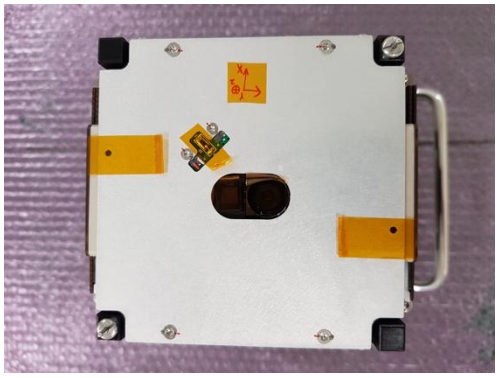

Fig. 17 Camera payload on the flight model, center of surface

5. Attitude Orbit Control System

5.1 Attitude control system

AV4 determines the attitude using sun sensors, gyroscope, and Kalman filter for the technological demonstration assuming only sun sensors are available on the lunar orbit. It depends on the initial condition and other factors, Kalman filter can estimate the attitude with single vector information, even its attitude determination is not solid compare to the static attitude determination of multiple vector information. For the future plan of actual lunar mission, additional sensor such as star sensor is under consideration.

For the AV4 in Earth orbit, the satellite position and reference time will be transferred from the ground stations using two-line element (TLE) set and current

UTC time when updates are needed. AOBA VELOX-IV has three reaction wheels. Two of the reaction wheels have momentum dumping using the PPT for the X and Y axes, but not for the Z axis due to limited space. Because of that, we performed several simulations to check the Z-axis reaction wheel saturation condition. If the initial angular velocity of deployment is small enough, less than 5 deg/s, and the environmental condition is not critical, the Z axis reaction wheel does not reach saturation within a short time of operation, at least one month, considering the execution of orbit correction and horizon observation maneuvers.

The momentum dumping of the reaction wheel has the function of evaluating how much performance the PPT has. The maximum angular speed of the reaction wheel is 4800 RPM in the nominal condition, and it has 0.004 kgm^2 for the moment of inertia of the wheel. The maximum momentum of the wheel is 0.002 Nmsec, and the PPT generates a torque of 1.0×10^{-6} Nm. If the PPT shows its design performance, it can dump the momentum of the wheel within 1 hour in orbit. Table 7 lists the AOCS operation modes. The AOCS algorithm is explained in depth in Ref. [29].

Table 7. AOCS operation modes

Operation mode	**Features**
Detumble mode	Reduction of angular rate via reaction wheels. This mode is used after AV4 deployment from launcher, or in the case of unusual increase of satellite angular velocity.
Sun-pointing mode	The solar paddles are aligned to the sun for optimal solar energy collection. During eclipse, the satellite attitude is not controlled.
Initialization mode	Initialization of orbit propagator and Extended Kalman Filter for attitude determination.
Science mode	The Z axis is aligned with the horizon and the mission camera points to the horizon to take the image. The velocity vector of satellite is aligned with the satellite Z axis for the demonstration of orbit maintenance function.
RW desaturation mode	PPTs provide torque to decrease the momentum of reaction wheels, leading to their desaturation until a low-limit speed is reached.

The function of the AOCS was first confirmed by the processor-in-the-loop simulator at Kyutech. It used an actual OBC with as much actual code as possible. Only the interface part was modified to exchange environmental information with

a Matlab Simulink simulator. AOCS showed stable attitude control performance in various conditions.

5.2 Processor-in-the-loop test

The final check of the AOCS was done at NTU by testing its performance on an air-bearing table, using the engineering model (EM) and a light source. The air-bearing table was placed inside a dark room in order to reduce the environmental light. At the beginning of the test procedures, EM downlink data was obtained through a wire for calibration purposes. Then, the NTU's mobile ground station and their mission control software were used to operate the EM and obtain the downlink data during the test procedures in wireless condition. In this way, we could verify the following features of the AOCS:

- Interface between AOCS software and OBC firmware
- Reaction wheels' spin direction according to the attitude control commands
- PPT commands for the desaturation of the reaction wheels in X and Y axes
- Calculation of the light source direction relative to the satellite body frame using coarse and fine sun sensors
- Attitude maneuvers for momentum dumping and alignment with the light source
- Sun tracking capability (by moving the light source to a different location)
- Initialization of the orbit propagator
- Initialization of the attitude determination based on Kalman Filter

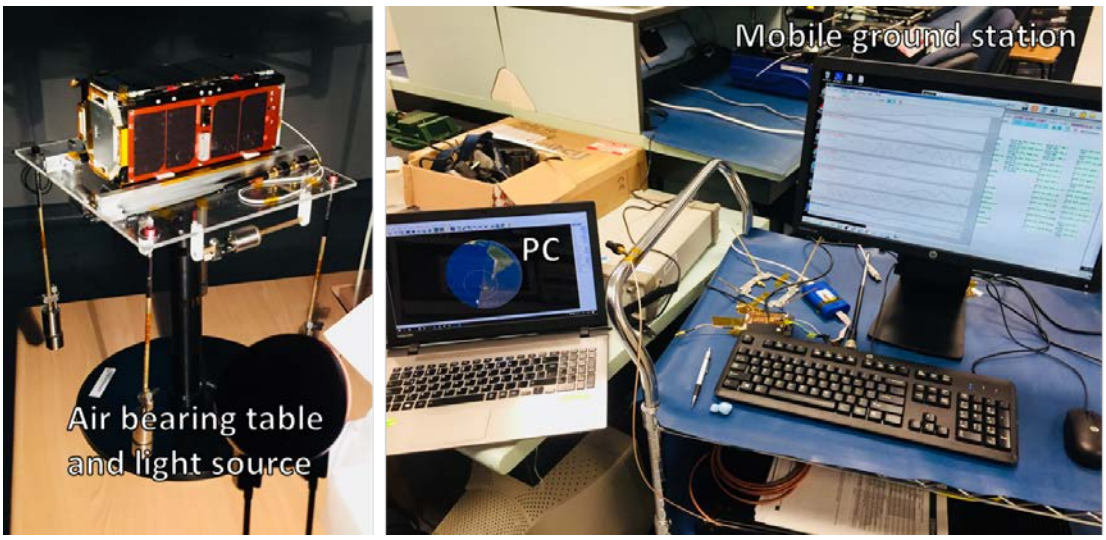

Fig. 18 AOCS verification process using the STM model

This test procedure allowed us to identify and solve issues related with the operation of the EM through AOCS commands from the mobile ground station. In

this way, the risk of an anomaly related with AV4 operation in orbit by using its AOCS was significantly reduced.

5.3 Orbit maintenance demonstration

The maximum ΔV of AOBA VELOX-IV is 60[m/sec] with the thruster of PPT. To measure the ΔV, the change in the satellite orbit elements must be measured with accuracy. Onboard GPS accuracy is enough to catch the change, however AV4 has no space for onboard GPS, the satellite's precise location needs to be analyzed by triangulation of the satellite signal. The satellite will be commanded from a ground station located at NTU of Singapore. A set of a software defined radio devices and a GPS clock will be distributed to ground stations near Singapore, such as Malaysia, Bangladesh, Philippines and Thailand. Those ground stations already form a network to operate the Kyutech BIRDS constellation satellites [30]. The ground stations measure the timing of satellite signal receiving based on the synchronized time with the GPS clock. From the relative time difference of the satellite signals measured at the multiple ground stations, the satellite position will be analyzed and the orbit elements will be derived with more accuracy from the TLE of NORAD.

6. Flight Model

The flight model already passed all the required tests for launch service in June 2018. Critical sub systems were examined before they were assembled on the flight model. One of the major critical safety items is the battery because it has a very high energy density. All the battery cells were screened to avoid defective cells, and the cells' characteristics were matched for the battery assembly module. The condition of each of the cells and the battery module was checked before they were assembled on the flight model. The check included a vacuum test, vibration test, shock test and charging-discharging test.

Another critical item was the deployment system. AV4 has deployable paddles for its solar cells and antenna. This kind of deployable system needed to be carefully confirmed to minimize the risk of hazard. For the deployment system, ultra-high molecular weight polyethylene string was used because of its high strength, high resistance to corrosive chemicals, low moisture absorption, very low friction coefficient, and high resistance to abrasion. This string was checked by two major tests, the creeping test and the strength test. The creeping test was to confirm that the length of string had no significant changes with high tension. High tension was applied to the four string samples using a mass of 0.168 kg. The length of string was periodically checked for more than 4 months. It showed that there was no significant change in length after 15 days, and its maximum change was 2% from the initial length. All strings of the flight model passed this creeping test to satisfy the initial installment length against the waiting time of the launch service. The string also needed to provide enough strength not to be cut by

accident. That strength was tested using a heavy load of 4.27 kg to apply triple the force of the nominal value of deployable force.

After the flight model was assembled, and before being shipped to Japan for the final environmental tests, AV4 went through a thermal vacuum test using the newly installed thermal vacuum chamber at NTU, as shown in Fig. 18. The thermal vacuum chamber had a cylindrical jar with a 900-mm diameter and 900-mm height (internal volume). The flight model was placed inside the chamber with its solar paddle stowed. The temperature was controlled at -10–50°C. The flight model went through 4 cycles of hot and cold soaks, where the hot soak was done at 50°C and the cold soak was done at -10°C. A cold start test of the satellite, as well as a deployment test, was conducted at -10°C. The functionality of the satellite flight model was completely checked through the thermal vacuum test.

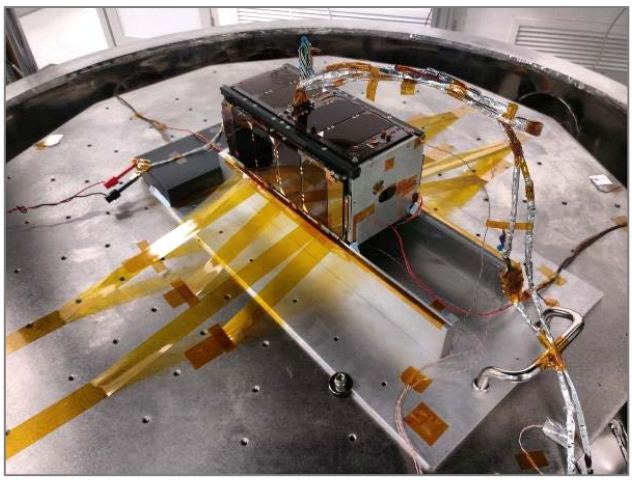

Fig. 19 Flight model in thermal vacuum chamber

After the flight model was shipped to Kyutech, AV4 first passed the following visual inspections:

- Fit check with the deployment POD for the rocket interface condition
- Vent hole size for safety
- No sharp edges for safety
- Double electrical insulation
- Connector pin layout
- Electrical grounding
- Visual check for rust on the structure

The AV4 flight model passed the vibration tests that included quasi-static load, sine wave vibration, and random vibration for each axis. The satellite was housed inside a newly developed POD system for the vibration. All the natural frequencies of the flight model were higher than 300 Hz, and no significant change was

observed due to the test. After the vibration test, the shock test was performed using the Kyutech test facility. The facility used compressed air to shoot a metal bullet to give the high-frequency shock to the test article. The shock response spectrum was checked to confirm that its level exceeded the required level, 587 G at 1000 Hz and above.

7. Conclusion

The lunar horizon glow mission of the AOBA VELOX project was introduced. The mission requirements, overall design, payloads, technical issues, and the flight model of AOBA VELOX-IV(AV4) have been presented. AV4 attempts to demonstrate the key technologies necessary for future lunar missions with a 2U CubeSat. It was quite challenging to put all the functionality into the body of a 2U CubeSat; however, the flight model had finally been completed and passed all the tests. Another challenge was to comply with the JAXA safety requirements, which led to significant design changes to the electrical power and antenna deployment systems. Compliance was verified by the environmental test of the flight model. The flight model had already been delivered to JAXA for the launch service and was launched to 500-km Sun-synchronous orbit on the Epsilon rocket in 18th January 2019. AV4 is still under initial operation, and does not finished all tests completely. After it was deployed in orbit, the housekeeping data have been checked to confirm the satellite's basic functions. After that, the performance of the four PPT heads have been checked with the AOCS, and several Earth-rim images and Earth night images were taken to demonstrate the imaging capability. The orbit maintenance capability demonstration is under schedule.

References

[1] Stubbs, T.J., Farrell, W.M., Halekas, J.S., Burchill, J.K., Collier, M.R., Zimmerman, M.I., Vondrak, R.R., Delory, G.T. and Pfaff, R.F. "Dependence of lunar surface charging on solar wind plasma conditions and solar irradiation" *Planetary and Space Science*, 90:10–27, 2014.

[2] Popel, S.I., Lisin, E.A., Izvekova, Y.N., Atamaniuk, B., Dolnikov, G.G., Zakharov, A.V. and Zelenyi, L.M. "Meteoroid impacts and dust particles in near-surface lunar exosphere" *Journal of Physics: Conference Series Journal of Physics: Conference Series*, 774(1):012175, 2016.

[3] Park, J. S., Liu, Y., Kihm, K. D. and Taylor, L. A. "Micro-morphology and toxicological effects of lunar dust" *37th Annual Lunar and Planetary Science Conference*, 37, 2006.

[4] Jaffe, L. D. "Depth of the lunar dust" *Journal of Geophysical Research*, *70*(24), 6129–6138, 1965.

[5] Rennilson, J. J. and Criswell, D. R. "Surveyor observations of lunar horizon-glow" *The Moon*, 10(2):121–142, 1974.

[6] Glenar, D. A., Stubbs, T. J., McCoy, J. E. and Vondrak, R. R. "A reanalysis of the Apollo light scattering observations, and implications for lunar exospheric dust" *Planetary and Space Science*, 59(14):1695–1707, 2011.

[7] Wang, X., Schwan, J., Hsu, H.W., Grün, E. and Horányi, M. "Dust charging and transport on airless planetary bodies" *Geophysical Research Letters*, 43(12):6103–6110, 2016.

[8] Schwan, J., Wang, X., Hsu, H.W., Grün, E. and Horányi, M. "The charge state of electrostatically transported dust on regolith surfaces" *Geophysical Research Letters*, 44(7):3059–3065, 2017.

[9] Orger, N. C., Alarcon, J. R. C., Toyoda, K., & Cho, M. "Lunar Dust Lofting due to Surface Electric Field and Charging within Micro-cavities between Dust Grains above the Terminator Region" *Advances in Space Research,* Vol. 62 (4), 896–911, 2018.

[10] Orger, N. C., Cordova-Alarcon, J. R., Toyoda, K. and Cho, M. "Investigation of Electrostatic Transportation of Lunar Dust Grains due to Ambient Plasma Conditions" *JAXA Special Publication: Proceedings of the 14th Spacecraft Environment Symposium Aerospace Exploration Agency Special*, 59–62, 2018.

[11] Glenar, D. A., Stubbs, T. J., Hahn, J. M. and Wang, Y. "Search for a high-altitude lunar dust exosphere using Clementine navigational star tracker measurements" *Journal of Geophysical Research: Planets*, 119(12):2548–2567, 2014.

[12] Horányi, M., Szalay, J.R., Kempf, S, Schmidt, J., Grün, E., Srama, R. and Sternovsky, Z. "A permanent, asymmetric dust cloud around the Moon" *Nature*, 522(7556):324–326, 2015.

[13] Szalay, J. R. and Horányi, M. "The search for electrostatically lofted grains above the Moon with the Lunar Dust Experiment" *Geophysical Research Letters*, 42(13):5141–5146, 2015.

[14] Poghosyan, A. and Golkar, A. "CubeSat evolution: Analyzing CubeSat capabilities for conducting science missions" *Progress in Aerospace Sciences,* Vol. 88, pp. 59–83, 2017.

[15] Mengu Cho, et al. “Technology Demonstration Mission for Lunar Horizon Glow Image Capture by a CubeSat; Overview of Aoba Velox-IV” *60th Space Science Technology Conference*, Hakodate, Japan, September 2016.

[16] Criswell, D. R. “Horizon-glow and the motion of lunar dust” *Photon and Particle Interactions with Surfaces in Space*, pp. 545–556. Springer, 1973.

[17] McCoy, J. E. “Photometric studies of light scattering above the lunar terminator from Apollo solar corona photography” *Lunar and Planetary Science Conference Proceedings*, pp. 1087–1112, 1976.

[18] Stubbs, T. J.,Vondrak, R. R. and Farrell, W. M. “A dynamic fountain model for lunar dust” *Advances in Space Research*, 37(1):59–66, 2006.

[19] Rennilson, J. J., & Criswell, D. R. “Surveyor observations of lunar horizon-glow” *The Moon*, 1974, 10(2), 121–142.

[20] Colwell, J. E., Batiste, S., Horányi, M., Robertson, S. and Sture, S. “Lunar surface: Dust dynamics and regolith mechanics” *Reviews of Geophysics*, 45(2):RG2006, 2007.

[21] McCoy, J. E. “Photometric studies of light scattering above the lunar terminator from Apollo solar corona photography” *Lunar and Planetary Science Conference Proceedings*, Vol. 7, pp. 1087–1112, April 1976.

[22] James D.Hale, Gemman Davies, Alison J. Faibass, Thomas J. Matthews, Christopher D. F. Rogers, Jon P. Sadler, “Mapping Lightscapes: Spatial Patterning of Artificial Lighting in an Urban Landscape”, *PLOS ONE*, Vol. 8, Issue 5, May 2013.

[23] Konopliv, A. S., Park, R. S., Yuan, D. N., Asmar, S. W., Watkins, M. M., Williams, J. G., Fahnestock, E., Kruizinga, G., Paik, M., Strekalov, D., Harvey, N., Smith D. E. and Zuber M. T. “The JPL lunar gravity field to spherical harmonic degree 660 from the GRAIL Primary Mission” *Journal of Geophysical Research: Planets*, 118 pp. 1–20, 2013.

[24] M. Lara “Design of long-lifetime lunar orbits: A hybrid approach” *Acta Astronautica* 69 (2011) 186–199. doi:10.1016/j.actaastro.2011.03.009.

[25] David Folta, David Quinn “Lunar frozen orbits” *AIAA/AAS Astrodynamics Specialist Conference and Exhibit*, Colorado, United States, 2006, pp. 1–18. doi: 10.2514/6.2006-6749.

[26] J. Rodrigo Cordova Alarcon, Necmi Cihan Örger, Sangkyun Kim, Tran Quang Vinh, Lim Wee Seng, Bui Tran Duy Vu, Mengu Cho “Moon Mission Lifetime

Analysis of a 2U CubeSat Equipped with Pulsed Plasma Thrusters; The Aoba-VELOX IV Mission Case" *26th International Symposium on Space Flight Dynamics ISSFD, 31th ISTS Conference*, Japan, 2017.

[27] A. Ruggiero, P. Pergola, S. Marcuccio, M. Andrenucci, "Low-thrust maneuvers for the efficient correction of orbital elements" *32nd International Electric Propulsion Conference*, Wiesbaden, Germany, 2011, pp. 1–13.

[28] R. D. Falck, W. K. Sjauw "Comparison of low-thrust control laws for application in planetocentric space" *50th AIAA/ASME/SAE/ASEE Joint Propulsion Conference*, American Institute of Aeronautics and Astronautics, Ohio, USA, 2011, pp. 1–14. doi:10.2514/6.2014-3714.

[29] Rodrigo Cordova-Alarcon J., et al. "Aoba VELOX-IV Attitude and Orbit Control System Design for a LEO Mission Applicable to a Future Lunar Mission" *67th IAC*, Guadalajara, IAC-16-A3.IP.33.x35734, Mexico, September 2016.

[30] Mengu Cho, Apiwat Jirawattanaphol, JGMNB project members, JGMNB partners, Naomi Kurahara, "Global network operations of CubeSats constellation*", 1st IAA Latin American Symposium on Small Satellites*, Buenos Aires, Argentina, March 2017.

[31] Roger M. Myers, Lynn A. Arrigton, Eric J. Pencil, Justin Carter, Jason Heminger, Nicolas Gatsonis, "Pulsed Plasma Thruster Contamination", 32nd Joint Propulsion Conference cosponsored by AIAA, ASME, SAE, and ASEE, Lake Buena Vista, Florida, July 1-3, 1996